



## RESEARCH LETTER

10.1002/2014GL062024

## Key Points:

- Snag attrition controls postfire albedo more than vegetation recovery
- Albedo perturbation was 14 times larger in winter compared to summer
- Negative radiative forcing increases linearly for at least 15 years postfire

## Supporting Information:

- Figures S1–S3

## Correspondence to:

T. L. O'Halloran,  
tohalloran@sbcc.edu

## Citation:

O'Halloran, T. L., S. A. Acker, V. M. Joerger, J. Kertis, and B. E. Law (2014), Postfire influences of snag attrition on albedo and radiative forcing, *Geophys. Res. Lett.*, 41, doi:10.1002/2014GL062024.

Received 26 SEP 2014

Accepted 17 NOV 2014

Accepted article online 20 NOV 2014

## Postfire influences of snag attrition on albedo and radiative forcing

Thomas L. O'Halloran<sup>1</sup>, Steven A. Acker<sup>2</sup>, Verena M. Joerger<sup>1</sup>, Jane Kertis<sup>3</sup>, and Beverly E. Law<sup>4</sup>

<sup>1</sup>Department of Environmental Science, Sweet Briar College, Sweet Briar, Virginia, USA, <sup>2</sup>U.S. Forest Service, Willamette National Forest, Springfield, Oregon, USA, <sup>3</sup>U.S. Forest Service, Siuslaw National Forest, Corvallis, Oregon, USA, <sup>4</sup>College of Forestry, Oregon State University, Corvallis, Oregon, USA

**Abstract** This paper examines albedo perturbation and radiative forcing after a high-severity fire in a mature forest in the Oregon Cascade Range. Correlations between postfire albedo and seedling, sapling, and snag (standing dead tree) density were investigated across fire severity classes and seasons for years 4–15 after fire. Albedo perturbation was 14 times larger in winter compared to summer and increased with fire severity class for the first several years. Albedo perturbation increased linearly with time over the study period. Correlations between albedo perturbations and the vegetation densities were strongest with snags, and significant in all fire classes in both summer and winter ( $R < -0.92$ ,  $p < 0.01$ ). The resulting annual radiative forcing at the top of the atmosphere became more negative linearly at a rate of  $-0.86 \text{ W m}^{-2} \text{ yr}^{-1}$ , reaching  $-15 \text{ W m}^{-2}$  in year 15 after fire. This suggests that snags can be the dominant controller of postfire albedo on decadal time scales.

### 1. Introduction

Climate change is predicted to increase the severity and/or frequency of ecosystem disturbances, including wildfire [Westerling *et al.*, 2006], drought [Williams and Funk, 2011], insect outbreaks [Raffa *et al.*, 2008], and severe storms [Bender *et al.*, 2010]. Large wildfire occurrence is increasing in the western United States [Dennison *et al.*, 2014] and is predicted to continue increasing as changing precipitation and temperature patterns increase the duration of the fire season [Westerling *et al.*, 2006; Yue *et al.*, 2013]. Similar patterns are expected in the circumpolar boreal forests [Flannigan *et al.*, 2009]. In boreal Canada, wildfire coverage is predicted to double in area under a  $3 \times \text{CO}_2$  scenario [Amiro *et al.*, 2009]. Ecosystem disturbances can feed back to climate by altering surface-atmosphere greenhouse gas and radiation exchange through several mechanisms. Net primary productivity is reduced when live photosynthetic tissue (e.g., leaf area) is reduced and transferred to dead pools, which enhances respiratory losses of carbon. Reduction in leaf area also affects surface reflectance if soils are exposed and bright (e.g., sandy), and in environments that experience snow [Huete *et al.*, 1985]. These effects vary across ecosystem and disturbance types and are dynamic in time [O'Halloran *et al.*, 2012].

To date, the majority of research on the climate impacts of ecosystem disturbances has focused on the greenhouse gas and albedo impacts of wildfire [Randerson *et al.*, 2006; Lyons *et al.*, 2008; Jin *et al.*, 2012a; Tsuyuzaki *et al.*, 2009; Jin and Roy, 2005; Rogers *et al.*, 2012]. Wildfire is perhaps the most severe disturbance type, because perturbations to the surface energy balance and effects on net carbon uptake are relatively large and occur almost instantaneously [Amiro *et al.*, 2010]. The magnitude of those changes and the recovery rate to prefire values vary widely across biomes. For example, in Australia, albedo perturbation (reduction) is proportional to fire severity, which increases as the dry season progresses [Jin and Roy, 2005]. In forested areas that experience snow, canopy removal by disturbance tends to increase albedo [Lyons *et al.*, 2008] since branches and foliage absorb radiation that would otherwise efficiently reflect off the high-albedo surface of underlying snow [Betts and Ball, 1997; Gleason *et al.*, 2013]. Other factors that alter postfire albedo include the vegetation destruction and the ash and charcoal left behind [Jin *et al.*, 2012a], differences in fuel combustion and consumption [Jin and Roy, 2005], and vegetation succession [Lyons *et al.*, 2008; Jin *et al.*, 2012b, 2012a; Randerson *et al.*, 2006]. In boreal fires in Alaska, postfire summer albedo increases have been attributed to early succession of grasses, herbaceous and deciduous species, and the recovery of surviving understory trees [Lyons *et al.*, 2008; Tsuyuzaki *et al.*, 2009; Randerson *et al.*, 2006; Jin *et al.*, 2012a]. Thus, most studies have focused on vegetation recovery in controlling postfire albedo, and to our knowledge, little attention has been paid to the potential importance of snag attrition.



**Figure 1.** Photo of a severe, crown-consumed region of the burn site in 2011, approximately 15 years after fire.

The number of standing dead trees (snags) created by forest disturbances depends on the density of preexisting trees, as well as disturbance type and severity. For example, high-severity fire may lead to 90–100% tree mortality, with low-stemwood combustion (<5%) and high-litter and foliage combustion (e.g., 100%) [Campbell *et al.*, 2007; Meigs *et al.*, 2009]. Low-severity fires may scorch tree boles without producing tree mortality [Campbell *et al.*, 2007; Meigs *et al.*, 2009]. Tree mortality often increases when insects and diseases attack trees weakened by fire in the years after fire occurrence. Tree mortality from mountain pine beetle infestation also ranges from near zero to total stand replacement, depending on the distribution of host species and ages [Shore *et al.*, 2006].

Snag fall rate (attrition rate) also varies greatly across landscapes and is strongly affected by salvage activities since harvest removes the larger snags. Snag attrition often begins after the first 3 years postdisturbance [Mitchell and Preisler, 1998; Russell *et al.*, 2006]. Older, more structurally damaged snags tend to fall faster than younger, less damaged snags [Huggard, 1999]. Other factors controlling snag attrition can include tree size [Bull, 1983], tree species [Landram *et al.*, 2002], mortality cause [Raphael and Morrison, 1987], soil type [Keen, 1955], stand density [Mitchell and Preisler, 1998], and wind events [Schmid *et al.*, 1985]. Half-lives (the time it takes for 50% attrition) of 5–15 years are typical in beetle and fire-killed coniferous trees in western North America [Harrington, 1996; Russell *et al.*, 2006], although large snags (>100 cm) stand for several decades [Bull, 1983; Cline *et al.*, 1980; Everett *et al.*, 2000].

In this study we use field surveys of vegetation after a fire, combined with Moderate Resolution Imaging Spectroradiometer (MODIS) albedo data, to evaluate the hypothesis that snag attrition exerts a significant control on albedo in addition to vegetation recovery following fire.

## 2. Methods

### 2.1. Site Description

The Charlton Fire occurred in August 1996, adjacent to Waldo Lake in the central Cascade Range of Oregon. The fire was caused by lightning and burned >3700 ha. Fire severity varied spatially, with >95% tree mortality occurring on most of the area [Salix Associates, 1998; Gardner and Whitlock, 2001] (Figure 1). The study area elevation is approximately 1700 m and typically has snow cover from mid-November until mid-June or later [Acker *et al.*, 2013]. Maximum snow depth at the nearby Irish Taylor Snotel site [United States Department of Agriculture Natural Resources Conservation Service, 2011], between 2006 and 2013 (the period

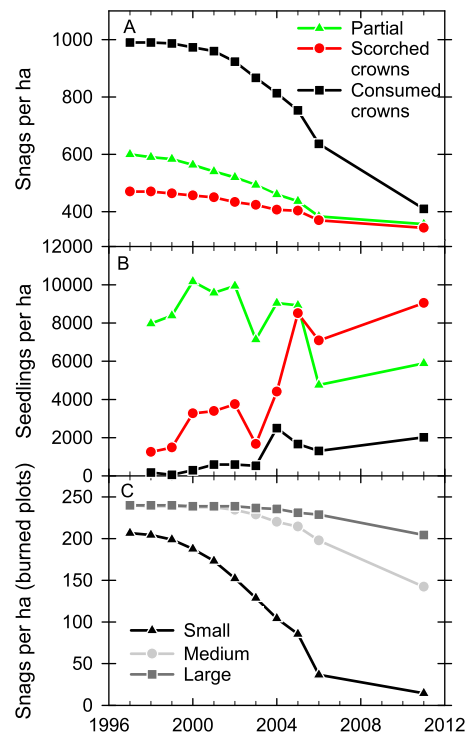


**Figure 2.** Time series of (a) snag and (b) seedling density within the three fire classes (partial burn; high severity, scorched crowns; high severity, consumed crowns). (c) Time series of snag density by size class, averaged across burned plots. The fire occurred in August 1996.

of record), averaged 2990 mm. Prefire vegetation in the area consisted of late successional evergreen needleleaf forest, dominated by mountain hemlock, with an understory of grouse huckleberry (*Vaccinium scoparium* Leib. ex Coville) and a sparse herbaceous layer [Salix Associates, 1998].

## 2.2. Field Measurements

We investigated the postfire dynamics of snags and tree regeneration across four fire severity classes: (1) unburned (>90% surviving trees), (2) partial mortality (>10% and <90% surviving trees), (3) high mortality, scorched crowns (<10% surviving trees), and (4) high mortality, consumed crowns (<10% surviving trees).

We used preexisting permanent plots and randomly located additional plots to sample three replicates of each fire severity class (12 plots total). Sampling occurred annually from 1997 through 2006, and again in 2011. Plots are circular with a 17.84 m (0.1 ha.) radius. Within each plot, we established two-belt transects,  $2 \times 14$  m each, divided into seven,  $2 \times 2$  m quadrats. In each quadrat we recorded the number and size of seedlings and saplings, while snags were measured over the entire 0.1 ha plot. Seedlings (<1.37 m tall) were tallied in 10 cm height classes and saplings in diameter classes up to 5 cm. Snags were grouped into three size classes based on diameter at breast high (DBH) (small: DBH < 14.9 cm; medium:  $14.9 \text{ cm} \leq \text{DBH} < 35.5 \text{ cm}$ ; large: DBH  $\geq 35.3 \text{ cm}$ ).

The pattern of canopy disturbance resulting from the Charlton Fire was characterized using postfire aerial

photographs, with interpretation aided by low-level flights over the area shortly after the fire [see Acker *et al.*, 2013, Figure 1].

## 2.3. MODIS Albedo

MODIS broadband shortwave blue-sky albedo data (MCD43A, 500 m spatial resolution) [Schaaf *et al.*, 2002] were extracted for a  $26.5 \times 26.5$  km area that encompassed the burn and adjacent unburned areas during years 2000–2011 using the MODIS subsetting tool [Oak Ridge National Laboratory Distributed Active Archive Center, 2014]. An aerosol optical depth of 0.2 was used in the calculation of blue-sky albedo [O'Halloran *et al.*, 2012; Loranty *et al.*, 2014], and data were only included that passed the quality control filters. Albedo data in the burn area were aggregated and averaged by fire severity class using the fire severity map [Acker *et al.*, 2013], which was downscaled to the same spatial resolution as the albedo data using bicubic interpolation. The resulting number of MODIS pixels available for each fire class was 12, 6, and 79 for partial burn, scorched crowns, and consumed crowns, respectively. Relative to FLUXNET tower measurements, MODIS Collection 5 shortwave albedo has a bias of  $-0.008$  and standard error of 0.023 [Wang *et al.*, 2010].

Control albedo values were produced by averaging albedo data in a  $2.5 \times 2.5$  km (25 pixel) area of unburned, mature forest, 4 km south of the burn. An albedo perturbation was calculated at each time step by subtracting the mean control albedo from the mean severity class albedo. Using a local, unburned site to provide control albedo values accounts for interannual variability in snow depth and timing, which is a strong control on albedo. For each albedo average, gaps in the 8 day time series were filled by averaging values linearly interpolated across gaps with values taken from the 12 year ensemble average for that fire severity class, which has the benefit of constraining the local information provided by the interpolation with phenological and climatological information included in the ensemble average. This helps reduce interpolation errors from the discontinuities caused at the edges of snowy periods, where the albedo changes abruptly [O'Halloran *et al.*, 2012; Loranty *et al.*, 2014]. For the radiative forcing calculations, the

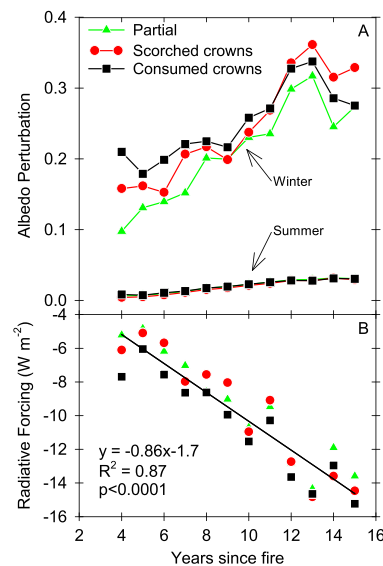


**Figure 3.** (a) Time series of MODIS albedo perturbation (burn minus control) in winter and summer in the three fire classes and (b) time series of resulting annual top of the atmosphere shortwave radiative forcing for each fire class with linear regression model and associated statistics.

8 day MODIS values were averaged to monthly resolution. Summer ( $180 \leq \text{day of year (DOY)} \leq 280$ ) and winter ( $340 \leq \text{DOY} \leq 366$ ;  $1 \leq \text{DOY} \leq 80$ ) albedo averages were also produced to quantify snow-free and snowy conditions, respectively.

#### 2.4. Radiative Forcing

The top-of-the-atmosphere (TOA) radiative forcing caused by the measured perturbations to surface albedo was calculated using the radiative kernel technique [Shell *et al.*, 2008; Soden *et al.*, 2008; O'Halloran *et al.*, 2012; Vanderhoof *et al.*, 2014]. The radiative kernel represents changes to TOA fluxes caused by incremental changes in monthly average surface albedo from present-day values at 2.5° resolution. It essentially represents a climatology of the sensitivity of TOA net shortwave radiation to incremental changes in albedo at the surface, neglecting feedbacks. The radiative forcing is then calculated at a monthly time step from perturbations in forest albedo caused by the disturbance relative to an undisturbed control stand. We report uncertainty ranges in the radiative forcing that include 10% for accuracy in albedo measurements and an additional 10% associated with the radiative kernel technique.

#### 2.5. Correlation Analysis

Pearson's correlation coefficient ( $R$ ) was used to examine the variance in annual postfire albedo perturbation explained by vegetation metrics. Statistical significance was set at  $\alpha = 0.05$ .

### 3. Results

#### 3.1. Fire and Biota Results

Snags dominated vegetation structure throughout the study period. One year after the fire, snag densities averaged 600, 470, and 900 per ha on partial, scorched-crown, and consumed-crown plots, respectively [Acker *et al.*, 2013]. Live trees were about half as abundant as snags on the partial mortality plots (347/ha) and were sparse (20/ha) to absent on the scorched-crown and consumed-crown plots [Acker *et al.*, 2013]. Initial snag attrition was slow, especially on partial mortality and scorched-crown plots, and dominated by small diameter snags (Figure 2c). By the end of the study period, snag density converged across fire classes to approximately 350–400 per ha (Figure 2a).

Vegetation regeneration consisted primarily of seedlings throughout the study period (Figure 2b). At year 15, seedling densities averaged between about 2000 and 9000 per ha, depending on fire severity class; sapling densities averaged about 200 per ha on both partial mortality and scorched-crown plots and were not detected on consumed-crown plots (data not shown). Seedling abundance increased on scorched-crown and consumed-crown plots and decreased on partial mortality plots over the course of the study. In year 15, the most abundant sizes of seedlings on partial mortality plots were 20 to 29 cm height, while sizes up to 9 cm in height were the most abundant in both scorched-crown and consumed-crown plots. The density of seedlings on the Charlton Fire is low in comparison to the nearby Warner Creek Fire, where observations were restricted to seedlings greater than 10 cm in height and at 14 years after fire ranged from 1530 to 392,000 per ha [Brown *et al.*, 2013].

#### 3.2. Albedo Results

The response of albedo following fire was significantly greater in winter than summer (Figure 3a and Figure S1 in the supporting information). The initial albedo perturbation in summer was nearly identical across burn severities, and only +0.006 at the start of the albedo record (4 years following fire) and increased gradually to +0.03 at 15 years after fire. Averaged over the fire severity classes, and the 12 years of available data, the albedo response was 14 times greater in winter (compared to summer) and peaked at +0.34 in year 13 after fire. For the first several years following fire, winter albedo perturbation varied across fire class,

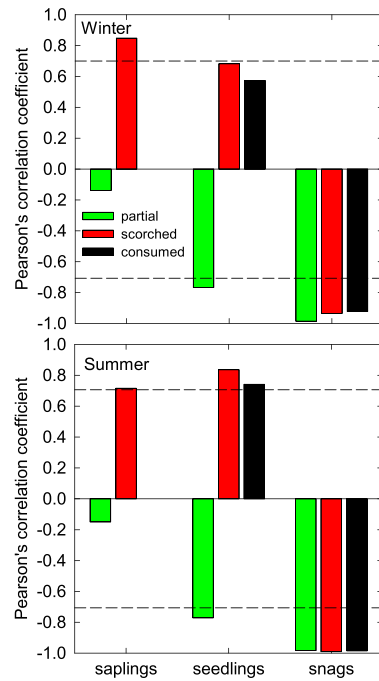


**Figure 4.** Pearson correlation coefficients between seasonal albedo perturbations and densities of saplings, seedlings, and snags for each fire class. Dashed lines indicate the threshold of significance at  $p < 0.05$ .

summer albedo perturbation only. This suggests that the increase in summer albedo is partially explained by the reestablishment of young vegetation, consistent with previous findings [Randerson *et al.*, 2006].

Seedling density increased the first few years after disturbance, and then decreased with time in partially burned areas, possibly due to higher root competition for water with surviving trees. Partial burn was the only area in which seedlings decreased after the first few years. Subsequently, albedo perturbation was significantly negatively correlated with seedling density in the partial burn. The only vegetation attribute exhibiting significant correlations with both summer and winter albedo perturbation in all three burn types was snags. These correlations were strongly negative and significant ( $R < -0.92$ ,  $p < 0.01$  in all cases).

#### 4. Discussion and Conclusions

The unburned mature mountain hemlock stand maintained very low albedo (~0.15) in winter even with significant snow on the ground. Removal of the canopy by fire initially increased albedo greatly during winter (e.g., +0.35 in consumed-crown areas) by exposing underlying snow to the atmosphere. Strikingly, we found that winter albedo then increased nearly monotonically for the rest of the data record, up to 15 years after fire. This increase strongly correlates with the density of snags, which decreased with time as snags fell (e.g.,  $R^2 = 0.97, 0.87$ , and  $0.85$  for partial burn, scorched crowns, and consumed crowns, respectively). Snags likely controlled winter albedo at this site because they provide the dominant absorbing surfaces when seedlings are short enough to be buried by snow, as they were during the study period. We hypothesize that winter albedo will continue to increase until seedlings and saplings are tall enough to extend above the snowpack and reach a density that decreases albedo more than any continued increase through snag attrition.

It is interesting to note that the subcanopy effect of fire is to decrease albedo through deposition of burned woody debris (BWD) onto the snow surface [Gleason *et al.*, 2013]. Combined with increased transmission of

with higher-fire severity corresponding with greater albedo perturbation. However, the winter perturbations converged by year 10 following fire.

The resulting TOA annual radiative forcings were not significantly different across fire severity classes (e.g., partial versus consumed crown: two-sided Student's  $T$  test;  $t = 0.855$ ;  $p = 0.402$ ) because summer albedo perturbations, which more heavily weight the annual forcing, were not significantly different across fire classes. The resulting annual radiative forcing (Figure 3b) was large, starting at approximately  $-6 \text{ W m}^{-2}$  in year 4 after fire and decreasing (becoming more negative) linearly by  $-0.86 \text{ W m}^{-2} \text{ yr}^{-1}$  thereafter (Figure 3b;  $R^2 = 0.87$ ,  $p < 0.001$ ). By year 15, values had reached approximately  $-15 \text{ W m}^{-2}$ .

#### 3.3. Albedo-Vegetation Correlations

While the winter and summer albedo perturbation varied significantly in magnitude, both exhibited a nearly monotonic increase over the 12 year period. Subsequently, correlations between albedo and vegetation metrics were similar between the two seasons (Figure 4; scatterplots are provided in Figures 2 and 3 in the supporting information).

Because albedo perturbations increased with time, positive correlations occurred when vegetation density also increased with time. Significant positive correlations existed between the number of saplings and albedo (summer and winter) in scorched-crown areas only. Seedlings in scorched-crown and consumed-crown areas were significantly correlated with

radiation to the snow surface, this accelerates snowmelt and impacts local hydrology [Gleason *et al.*, 2013; Winkler, 2011]. However, from the perspective of the atmosphere, the increased reflectance from removing the canopy and exposing the snow surface greatly outweighs any snow darkening from BWD. Additionally, this effect only occurs during the snow ablation period, because fresh snow buries BWD during the period of snow accumulation.

While previous studies have documented albedo increases during snowy periods in the years following fire [Lyons *et al.*, 2008; Jin *et al.*, 2012a], and hypothesized that “losses of standing dead boles” may explain such observations [Jin *et al.*, 2012b], none have presented simultaneous observations of albedo and snags to test this hypothesis. In the interior of Alaska, decadal averages of early spring albedo increased to a peak in years 21–30 after fire [Lyons *et al.*, 2008]. Ongoing measurements of snag longevity within this region (near Delta Junction) suggest that snags fall at an average rate of 4% per year, leading to a half-life of approximately 12 years (K. Manies, personal communication, 2014). Over a very large latitudinal transect of central Canada, Jin *et al.* [2012a] found early spring albedo increased for 9 years after fire in the southern zone, and 14 years in the northern zone. Corresponding changes in enhanced vegetation index suggested vegetation recovered much faster in the southern area, leading to an earlier onset of the declining period in albedo. This supports our hypothesis that postfire snow-influenced albedo is controlled by a balance of recovering vegetation, which tends to lower albedo, and snag attrition, which tends to increase it.

Other studies of postfire snag persistence in coniferous or mixed coniferous-hardwood forests in North America have demonstrated rates of persistence similar [Chambers and Mast, 2005; Russell *et al.*, 2006; Brown *et al.*, 2013] to somewhat less [Angers *et al.*, 2011; Ritchie *et al.*, 2013] than those we observed. Large snags tend to persist longer, and species can differ significantly in their tendency to remain standing [Chambers and Mast, 2005; Russell *et al.*, 2006; Angers *et al.*, 2011; Brown *et al.*, 2013; Ritchie *et al.*, 2013]. For example, on the east slope of the Cascade Range in Washington State, longevity of snags <41 cm diameter was greater for subalpine fir and lodgepole pine than for Douglas fir, but for larger snags, Douglas fir was more persistent than other species [Everett *et al.*, 2000]. Thus, we hypothesize that snag control of albedo during the snowy season could be a common, but mostly overlooked, consequence of wildfires in boreal and temperate forests, particularly where fires burn larger trees of species likely to persist as snags (e.g., *Populus tremuloides* [Angers *et al.*, 2011] and *Pseudotsuga menziesii* [Russell *et al.*, 2006; Brown *et al.*, 2013]).

Several geographic factors contribute to making this, to our knowledge, the largest (most negative) fire-induced albedo radiative documented forcing to date. The value presented here is nearly double that reported by Randerson *et al.* [2006] for a fire in Alaska. This is mostly attributable to significantly higher average insolation at our midlatitude site (2.48 versus 4.28 kW h m<sup>-2</sup> d<sup>-1</sup>, NASA Surface meteorology and Solar Energy <https://eosweb.larc.nasa.gov/>). The snow period at this elevation is approximately 240 days, compared to 140–240 days for the majority of global boreal forests [Ménégoz *et al.*, 2013]. This causes high values of radiative forcing in the spring months, when snow is still lying and insolation is increasing. While this case probably represents a near upper bound on the magnitude of albedo radiative forcing caused by wildfire in forests, we note that the lower values of radiative forcing typically found in boreal regions are likely more significant to climate because they occur over a larger area.

Similar to fire, mountain pine beetle outbreaks also generate large numbers of snags that persist from 5 to 15 years on average [Mitchell and Preisler, 1998]. Measured increases in winter albedo following beetle outbreaks have also been attributed to snag attrition, suggesting this mechanism is not specific to fire [O'Halloran *et al.*, 2012; Vanderhoof *et al.*, 2014].

It is well established that snag attrition after fire is a large source of downed coarse woody debris and therefore an important control on the forest carbon balance for decades after fire (see review by Harmon *et al.* [2011]). The importance of snags and burned woody debris in controlling snowmelt and hydrology has also recently been shown [Gleason *et al.*, 2013]. Since we show that snag attrition additionally exerts a strong control on surface albedo (and therefore the surface energy balance) after fire, we suggest that snag attrition is a key process that should be included in coupled land-atmosphere models as they attempt to represent the climate impacts of forest disturbances, such as wildfire and insect outbreaks.

## Acknowledgments

We thank Matthew Blakeley-Smith, Sarah Greene, Becky Fasth, Shea McKusick, Rob Pabst, Alison Shapiro, Travis Wooley, and many others for dedicated fieldwork. Thanks to Rob Pabst for data management and coordinating fieldwork. We thank two anonymous reviewers for feedback that improved the manuscript. This work was funded by grants from the U.S. Department of Energy (DOE), Office of Science (BER), contract DE-FG02-06ER64318 for AmeriFlux research, The National Science Foundation to the Andrews Experimental Forest Long-Term Ecological Research Program (DEB-96-32921, DEB-0218088, and DEB-0823380), cooperative agreements between the Pacific Northwest Research Station of the U.S. Forest Service and Oregon State University, and an interagency agreement between the U.S. Forest Service and the National Park Service. Plot data are available from <http://andrewsforest.oregonstate.edu/> under study code TV045. MODIS data used in this study are freely available at <http://daac.ornl.gov/MODIS/modis.shtml>.

The Editor thanks two anonymous reviewers for their assistance in evaluating this paper.

## References

- Acker, S. A., J. Kertis, H. Bruner, K. O'Connell, and J. Sexton (2013), Dynamics of coarse woody debris following wildfire in a mountain hemlock (*Tsuga mertensiana*) forest, *For. Ecol. Manage.*, *302*, 231–239.
- Amiro, B. D., A. Cantin, M. D. Flannigan, and W. J. de Groot (2009), Future emissions from Canadian boreal forest fires, *Can. J. For. Res.*, *39*, 383–385.
- Amiro, B. D., et al. (2010), Ecosystem carbon dioxide fluxes after disturbance in forests of North America, *J. Geophys. Res.*, *115*, G00K02, doi:10.1029/2010JG001390.
- Angers, V. A., S. Gauthier, P. Drapeau, K. Jayen, and Y. Bergeron (2011), Tree mortality and snag dynamics in North American boreal tree species after a wildfire: A long-term study, *Int. J. Wildland Fire*, *20*, 751–763.
- Bender, M. A., T. R. Knutson, R. E. Tuleya, J. J. Sirutis, G. A. Vecchi, S. T. Garner, and I. M. Held (2010), Modeled impact of anthropogenic warming on the frequency of intense Atlantic hurricanes, *Science*, *327*, 454–458.
- Betts, A. K., and J. H. Ball (1997), Albedo over the boreal forest, *J. Geophys. Res.*, *102*(D24), 28,901–28,909.
- Brown, M. J., J. Kertis, and M. H. Huff (2013), Natural tree regeneration and coarse woody debris dynamics after a forest fire in the Western Cascade Range, *Res. Pap. PNP-RP-592*, 50.
- Bull, E. L. (1983), Longevity of snags and their use by woodpeckers, *Forest*, *1975*, 82.
- Campbell, J., D. Donato, D. Azuma, and B. Law (2007), Pyrogenic carbon emission from a large wildfire in Oregon, United States, *J. Geophys. Res.*, *112*, G04014, doi:10.1029/2007JG000451.
- Chambers, C. L., and J. N. Mast (2005), Ponderosa pine snag dynamics and cavity excavation following wildfire in northern Arizona, *For. Ecol. Manage.*, *216*, 227–240.
- Cline, S. P., A. B. Berg, and H. M. Wight (1980), Snag characteristics and dynamics in Douglas-fir forests, western Oregon, *J. Wildl. Manage.*, *44*, 773–786.
- Dennison, P. E., S. C. Brewer, J. D. Arnold, and M. A. Moritz (2014), Large wildfire trends in the western United States, 1984–2011, *Geophys. Res. Lett.*, *41*, 2928–2933, doi:10.1002/2014GL059576.
- Everett, R., J. Lehmkuhl, R. Schellhaas, P. Ohlson, D. Keenum, H. Riesterer, and D. Spurbeck (2000), Snag dynamics in a chronosequence of 26 wildfires on the east slope of the Cascade Range in Washington State, USA, *Int. J. Wildland Fire*, *9*(4), 223–234.
- Flannigan, M. D., M. A. Krawchuk, W. J. de Groot, B. M. Wotton, and L. M. Gowman (2009), Implications of changing climate for global wildland fire, *Int. J. Wildland Fire*, *18*, 483–507.
- Gardner, J. J., and C. Whitlock (2001), Charcoal accumulation following a recent fire in the Cascade Range, northwestern USA, and its relevance for fire-history studies, *The Holocene*, *11*(5), 541–549.
- Gleason, K. E., A. W. Nolin, and T. R. Roth (2013), Charred forests increase snowmelt: Effects of burned woody debris and incoming solar radiation on snow ablation, *Geophys. Res. Lett.*, *40*, 4654–4661, doi:10.1002/grl.50896.
- Harmon, M. E., B. Bond-Lamberty, J. Tang, and R. Vargas (2011), Heterotrophic respiration in disturbed forests: A review with examples from North America, *J. Geophys. Res.*, *116*, 1–17, doi:10.1029/2010JG001495.
- Harrington, M. (1996), Fall rates of prescribed fire-killed ponderosa pine, *Forest Serv. Res. Pap.*
- Huete, A., R. Jackson, and D. Post (1985), Spectral response of a plant canopy with different soil backgrounds, *Remote Sens. Environ.*, *17*(1), 37–53.
- Huggard, D. J. (1999), Static life-table analysis of fall rates of subalpine fir snags, *Ecol. Appl.*, *9*(3), 1009–1016.
- Jin, Y., and D. P. Roy (2005), Fire-induced albedo change and its radiative forcing at the surface in northern Australia, *Geophys. Res. Lett.*, *32*, L13401, doi:10.1029/2005GL022822.
- Jin, Y., J. T. Randerson, M. L. Goulden, and S. J. Goetz (2012a), Post-fire changes in net shortwave radiation along a latitudinal gradient in boreal North America, *Geophys. Res. Lett.*, *39*, L13403, doi:10.1029/2012GL051790.
- Jin, Y., J. T. Randerson, S. J. Goetz, P. S. A. Beck, M. M. Lorant, M. Michael, and M. L. Goulden (2012b), The influence of burn severity on postfire vegetation recovery and albedo change during early succession in North America boreal forests, *J. Geophys. Res.*, *117*, G01036, doi:10.1029/2011JG001886.
- Keen, F. P. (1955), The rate of natural falling of beetle-killed ponderosa pine snags, *J. For.*, *53*, 720–723.
- Landram, F. M., W. F. Laudenslayer Jr., and T. Atzet (2002), Demography of Snags in Eastside Pine Forests of California, *USDA Forest Service Gen. Tech. Rep. PSW-GTR-181*, pp. 605–620. [Available at [http://www.fs.fed.us/psw/publications/documents/gtr-181/046\\_Landram.pdf](http://www.fs.fed.us/psw/publications/documents/gtr-181/046_Landram.pdf).]
- Lorant, M. M., L. T. Berner, S. J. Goetz, Y. Jin, and J. T. Randerson (2014), Vegetation controls on northern high latitude snow-albedo feedback: Observations and CMIP5 model simulations, *Global Change Biol.*, *20*, 594–606.
- Lyons, E. A., Y. Jin, and J. T. Randerson (2008), Changes in surface albedo after fire in boreal forest ecosystems of interior Alaska assessed using MODIS satellite observations, *J. Geophys. Res.*, *113*, G02012, doi:10.1029/2007JG000606.
- Meigs, G. W., D. C. Donato, J. L. Campbell, J. G. Martin, and B. E. Law (2009), Forest fire impacts on carbon uptake, storage, and emission: The role of burn severity in the Eastern Cascades, Oregon, *Ecosystems*, *12*, 1246–1267.
- Ménégoz, M., G. Krinner, Y. Balkanski, A. Cozic, O. Boucher, and P. Ciais (2013), Boreal and temperate snow cover variations induced by black carbon emissions in the middle of the 21st century, *The Cryosphere*, *7*, 537–554.
- Mitchell, R. G., and H. K. Preisler (1998), Fall rate of lodgepole pine killed by the mountain pine beetle in central Oregon, *West. J. Appl. For.*, *13*(1), 23–26.
- Oak Ridge National Laboratory Distributed Active Archive Center (2014), MODIS subsetted land products, Collection 5, ORNL DAAC, Oak Ridge, Tenn. [Available at <http://daac.ornl.gov/MODIS/modis.html>, Accessed 15 Nov. 2012.]
- O'Halloran, T. L., B. E. Law, M. L. Goulden, Z. Wang, J. G. Barr, C. Schaaf, M. Brown, J. D. Fuentes, M. Göckede, and A. Black (2012), Radiative forcing of natural forest disturbances, *Global Change Biol.*, *18*, 555–565.
- Raffa, K. F., B. H. Aukema, B. J. Bentz, A. L. Carroll, J. A. Hicke, M. G. Turner, and W. H. Romme (2008), Cross-scale drivers of natural disturbances prone to anthropogenic amplification: The dynamic of bark beetle eruptions, *BioScience*, *58*, 501.
- Randerson, J., H. Liu, M. Flanner, S. Chambers, Y. Jin, P. Hess, G. Pfister, M. Mack, K. Treseder, and L. Welp (2006), The impact of boreal forest fire on climate warming, *Science*, *314*, 1130–1132.
- Raphael, M. G., and M. L. Morrison (1987), Notes: Decay and dynamics of snags in the Sierra Nevada, California, *For. Sci.*, *33*(3), 774–783.
- Ritchie, M. W., E. E. Knapp, and C. N. Skinner (2013), Snag longevity and surface fuel accumulation following post-fire logging in a ponderosa pine dominated forest, *For. Ecol. Manage.*, *287*, 13–122.
- Rogers, B., J. Randerson, and G. Bonan (2012), High latitude cooling associated with landscape changes from North American boreal forest fires, *Biogeosciences Discuss.*, *9*, 12,087–12,136.
- Russell, R. E., V. A. Saab, J. G. Dudley, and J. J. Rotella (2006), Snag longevity in relation to wildfire and postfire salvage logging, *For. Ecol. Manage.*, *232*, 179.

- Salix Associates (1998), Establishment record for Torrey-Charlton Research Natural Area, *Willamette National Forest*.
- Schaaf, C. B., et al. (2002), First operational BRDF, albedo nadir reflectance products from MODIS, *Remote Sens. Environ.*, *83*, 135–148, doi:10.1016/S0034-4257(02)00091-3.
- Schmid, J., S. Mata, and W. F. McCambridge (1985), *Natural Falling of Beetle-Killed Ponderosa Pine*, vol. 454, USDA Forest Service, Rocky Mountain Forest and Range Experiment Station.
- Shell, K. M., J. T. Kiehl, and C. A. Shields (2008), Using the radiative kernel technique to calculate climate feedbacks in NCAR's community atmospheric model, *J. Clim.*, *21*, 2269–2282, doi:10.1175/2007jcli2044.1.
- Shore, T. L., L. Safranyik, B. C. Hawkes, and S. W. Taylor (2006), Effects of the mountain pine beetle on lodgepole pine stand structure and dynamics, in *The Mountain Pine Beetle: A Synthesis of Biology, Management, and Impacts on Lodgepole Pine*, edited by L. Safranyik and B. Wilson, Natural Resources Canada, Canadian Forest Service, Pacific Forestry Centre, Victoria, BC, 95–116.
- Soden, B. J., I. M. Held, R. Colman, K. M. Shell, J. T. Kiehl, and C. A. Shields (2008), Quantifying climate feedbacks using radiative kernels, *J. Clim.*, *21*, 3504–3520, doi:10.1175/2007jcli2110.1.
- Tsuyuzaki, S., K. Kushida, and Y. Kodama (2009), Recovery of surface albedo and plant cover after wildfire in a *Picea mariana* forest in interior Alaska, *Clim. Change*, *93*, 517–525.
- United States Department of Agriculture Natural Resources Conservation Service (2011), Irish Taylor Snotel. [Available at <http://www.wcc.nrcs.usda.gov/nwcc/site?sitenum=545>, 2013.]
- Vanderhoof, M., C. A. Williams, Y. Shuai, D. Jarvis, D. Kulakowski, and J. Masek (2014), Albedo-induced radiative forcing from mountain pine beetle outbreaks in forests, south-central rocky mountains: Magnitude, persistence, and relation to outbreak severity, *Biogeosciences*, *11*, 563–575.
- Wang, K. C., S. Liang, C. L. Schaaf, and A. H. Strahler (2010), Evaluation of moderate resolution imaging spectroradiometer land surface visible and shortwave albedo products at FLUXNET sites, *J. Geophys. Res.*, *115*, doi:10.1029/2009JD013101.
- Westerling, A. L., H. G. Hidalgo, D. R. Cayan, and T. W. Swetnam (2006), Warming and earlier spring increase western U.S. forest wildfire activity, *Science*, *313*, 940–943, doi:10.1126/science.1128834.
- Williams, A. P., and C. Funk (2011), A westward extension of the warm pool leads to a westward extension of the walker circulation, drying eastern Africa, *Clim. Dyn.*, *37*, 2417–2435.
- Winkler, R. D. (2011), Changes in snow accumulation and ablation after a fire in south-central British Columbia, *Streamline Watershed Manage Bull.*, *14*, 1–7.
- Yue, X., L. J. Mickley, J. A. Logan, and J. O. Kaplan (2013), Ensemble projections of wildfire activity and carbonaceous aerosol concentrations over the western United States in the mid-21st century, *Atmos. Environ.*, *77*, 767–780, doi:10.1016/j.atmosenv.2013.06.003.